Illumination-Induced Modifications of Langmuir−Blodgett Films Consisting of a Deuterated Poly(vinyl alcohol) Having an Azobenzene Side Chain Transferred at Varied Packing Density

Takahiro Seki* and Kunihiro Ichimura

Research Laboratory of Resources Utilization, Tokyo Institute of Technology, 4259 Nagatsuta, Midori-ku, Yokohama 226, Japan

Ryo-ichi Fukuda, Takanobu Tanigaki, and Takashi Tamaki

National Institute of Materials and Chemical Research, 1-1 Higashi, Tsukuba, Ibaraki 305, Japan

Received August 28, 1995; Revised Manuscript Received October 31, 1995[⊗]

ABSTRACT: Langmuir−Blodgett (LB) films consisting of an amphiphilic azobenzene (Az) polymer having a deuterated poly(vinyl alcohol) were prepared at varied lateral Az packing density, and their initial and light-modulated structures were evaluated by X-ray reflectometry and Fourier-transform infrared (FT-IR) spectroscopy. X-ray reflectometry indicated that the layer structure of the LB film is strongly dependent on the lateral packing density. The more densely packed film was characterized by the better-defined structure in terms of the order of the local lamellar patterns and surface smoothness of the total film. The overall film thickness decreased and increased upon exposure to UV and visible light, respectively; however, the lamellar structure was irreversibly disordered by the first exposure to UV light. The deuterated PVA chain was found to have no appreciable orientational preference in the in-plane direction, as proven by polarized transmission FT-IR, although a nematic liquid crystal (LC) placed on these LB films exhibited a definitive homogeneous in-plane alignment depending on the Az packing density [Seki, T.; et al. *Thin Solid Films* **1994**, *243*, 675]. UV light (365 nm) irradiation on the LB films induced a tilt of the alkyl part in the Az side chain from the surface normal. The time course observation of the UV light induced changes in the IR signals revealed that the motion of the alkyl part in the most densely packed LB film was retarded from that of the Az aromatic rings. The IR signals from the alkyl part reverted to the original state on subsequent visible light (436 nm) illumination, but reproducibility of the signals from the aromatic ring was poor. Finally, an increase in the Az packing density substantially retarded the response of the UV light induced homeotropic → planar alignment change of a nematic LC placed on these Az LB films. The retarding effect was more manifest in this intermolecularly driven system.

1. Introduction

Langmuir−Blodgett (LB) films of photochromic azobenzene (Az) have been attracting increasing attention due to its diverse photofunctional applications such as photon-mode optical memories,[1−6] transducing optical information,[7] photoswitching of electron conductivity[8] and electrochemical properties,[9] and so forth. Many recent works have been devoted to light-induced structural and orientational modifications of Az LB films.[1−7] Apart from their photofunctionality, the structural characterization has been extensively carried out due to their particular utility in evaluations by means of UV−visible and infrared spectroscopic methods.[10−15]

We have been investigating LB films composed of poly(vinyl alcohol) derivatives (6Azn-PVA; see Chart 1) having Az side chains.[16,17] In these LB films, the polymer backbone prevents Az aggregation to some extent and therefore provides highly photoreactive LB films. Due to their high photoreactivity they can be utilized as the efficient " command surface" with which photochemical alignment switching of nematic liquid crystals (LCs) between the homeotropic and planar modes is feasible.[18−20] Regarding studies on structural characterization of these films, Katayama et al.[21] have conducted an extensive FT-IR study of 6Az1-PVA LB films and discussed the molecular orientation, anisotropy, and LC orientation on these LB layers. Waveguide spectroscopy has been applied to the 6Az10-PVA/nematic LC systems by Knobloch et al.[22] They presented experiments on the dynamics of the photoinduced LC orientation process and reported a continuous transition character of this surface-mediated process. Furthermore, Sekkat et al.[23] carried out the same measurements, particularly focusing on the sensitivity to the linearly polarized light illumination.

Chart 1

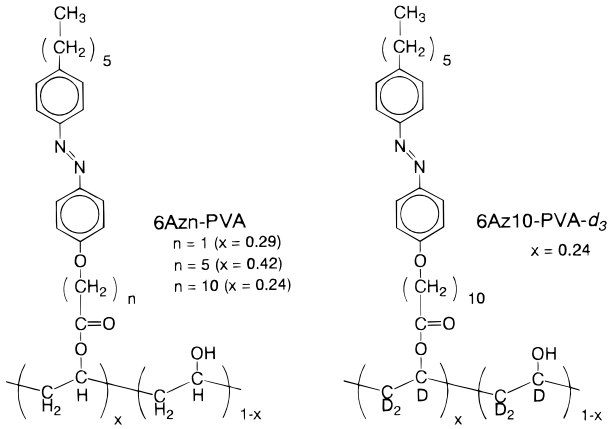

Our recent investigation revealed that the design of the surface Az layer, in particular the packing density of the layer, strongly influences the photoresponding behavior. For a 6Az10-PVA LB layer, the LB monolayers can be assorted into four separate regimes on the basis of the LC photoresponse and orientational nature.[20] For example, an orientational inversion of

[⊗] Abstract published in *Advance ACS Abstracts,* December 15, 1995.

0024-9297/96/2229-0892$12.00/0

nematic LC molecules regarding the dipping direction occurs in the area between 0.35 and 0.30 nm^2 per Az unit. This packing density-dependent behavior should be closely related to structural features of the LB films, and it seemed of particular importance to undertake a study of the structural justification of these LB films prepared at various packing densities. We report in this paper on the structural features of 6Az10-PVA-d_3 LB films with varied lateral packing density, and their light-induced modifications explored by means of X-ray reflectometry and Fourier transform infrared (FT-IR) spectroscopy. As an attempt to evaluate the main chain orientation, the backbone of 6Az10-PVA in this study is substituted by a deuterated PVA (6Az10-PVA-d_3, Chart 1) to separate the IR signals from the alkyl part in the PVA main chain and the Az side chains.

2. Experimental Section

2.1. Materials. All organic reagents for syntheses were purchased from Tokyo Kasei Kogyo Co. Deuterated poly(vinyl alcohol) (degree of polymerization = 2200) was the generous gift from Prof. Kazuaki Sakota of the Research Institute for Electronic Science at Hokkaido University.

11-[[4-[(4-Hexylphenyl)azo]phenyl]oxy]undecanoic acid (6Az10COOH) was synthesized as previously reported.[18]

6Az10-PVA-d_3 was synthesized essentially according to the previous paper for 6Az10-PVA.[18] The detailed procedures are as follows. The deuterated PVA (40 mg, 0.9 unit mmol) was dissolved in dry *N*,*N*-dimethylacetamide (DMAc, 2 mL) on heating. Another DMAc solution (3 mL) containing 6Az10COOH (0.467 g, 1.0 mmol), 2,4,6-trinitrochlorobenzene (0.273 g, 1.0 mmol), pyridine (0.237 g, 3.0 mmol), and a small portion of 4-(*N*,*N*-dimethylamino)pyridine (0.01 g) was added to the polymer solution. The mixture was heated at 100 °C for 3 h. After cooling to room temperature, the polymer solution was poured into 600 mL of methanol at 40 °C to obtain a yellow precipitate of the polymeric product (0.3 g, 69% yield). TLC on silica gel using ethyl acetate gave a product spot at R_f = 0.0, in contrast to 6Az10COOH at R_f = 0.7. The degree of esterification was determined photometrically using a molar extinction coefficient of 6Az10COOH at 352 nm (see Figure 2). The amount of the introduced Az chain (x in Chart 1) was 0.24, which is exactly consistent with that of 6Az10-PVA.[18]

2.2. Methods. Monolayer Experiments and LB Transfer. Observation of the spreading behavior of 6AZ10-PVA-d_3 and LB film preparation were carried out as previously described.[18]

Photoirradiation for LB film preparation was performed with a 500-W superhigh-pressure Hg lamp (Ushio UI-502Q). UV (365 nm) and visible (436 nm) light selected through Corning glass filters. For monitoring the UV light induced FT-IR and the LC alignment changes, a 150-W xenon lamp (Hamamatsu Photonics, Model C4251/C4264) was commonly used. The exposure energy at 365 nm for the latter experiments was 0.9 mW cm^{-2} at the sample.

UV−visible absorption spectra of Az monolayers on a quartz substrate were recorded on a JASCO HSSP-3 spectrophotometer.

FT-IR spectra in the transmission mode were taken on a Biorad FTS-60A equipped with an MCT detector in CO_2 free dry air. Transmission spectra of 1024 scans at the resolution of 1 cm^{-1} were accumulated and averaged. For the polarized spectrum measurements, a Biorad polarizer attachment was used. LB films of 6Az10-PVA-d_3 were deposited onto a CaF_2 crystal plate (10 × 30 × 1 mm, OKEN) for these measurements.

The X-ray diffraction profile in the reflection geometry was obtained with a Rigaku RU-300 at room temperature. The specimens were scanned at 0.2°/min using Cu Kα radiation monochromatized by pyrolyzed graphite.

Fabrication of the LC cell was reported in the previous paper.[18] 6Az10-PVA-d_3 was transferred as a single monolayer on a clean quartz plate. The photoinduced changes of a nematic LC (DON-103, Rodic Co.) alignment were monitored by observing the transmittance changes of an anthraquinone type dichroic dye dissolved (1% by weight) in the LC phase.

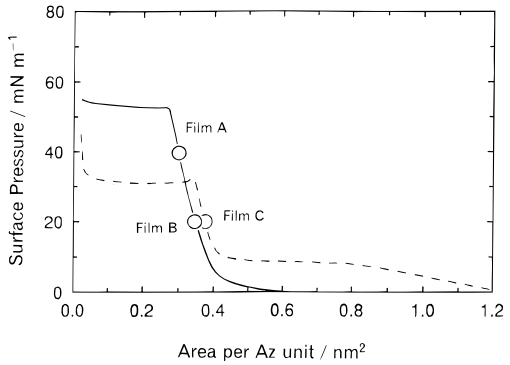

Figure 1. Surface pressure−area isotherms of the 6Az10-PVA-d_3 monolayer on pure water at 21 °C. Solid and broken curves indicate data for the visible light (436 nm) pre-irradiated (ca. 90% *trans*) and UV light (365 nm) pre-irradiated monolayers, respectively. Circles indicate the deposition conditions.

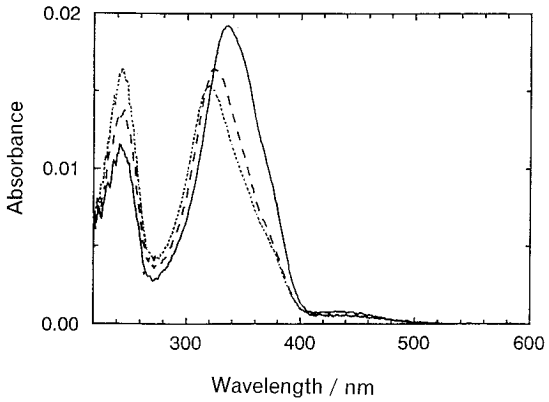

Figure 2. UV−visible absorption spectra of 6Az10-PVA-d_3 LB monolayers on both sides of a quartz plate. Solid, broken, and dotted lines indicate spectra of film C, film B, and film A, respectively.

3. Results

3.1. Spreading Behavior of Monolayer and LB Deposition. The surface pressure−area curves of 6Az10-PVA-d_3 monolayer at 20 °C are displayed in Figure 1. The characteristics of the curves in terms of the molecular limiting area, the surface pressure, collapse pressure, and magnitude of expansion in the UV-irradiated monolayer are in close agreement with those for 6Az10-PVA reported previously.[20] LB films were prepared under three area conditions: (a) 0.30 nm^2 per Az unit at 40 mN m^{-1} (film A) and (b) 0.35 nm^2 at 20 mN m^{-1} (film B) from a 436-nm light pre-irradiated monolayer and (c) 0.38 nm^2 at 20 mN m^{-1} from a 365 nm-light pre-irradiated monolayer (film C). The deposition conditions are indicated as the circles in the figure with notations of films A−C. These deposition conditions were chosen on the basis of the previous results[20] that the orientational nature of LC molecules drastically changes around these conditions. Films A−C could be deposited in the Y-type mode at satisfactory transfer ratios (>0.9).

In addition to the spreading behavior, features of UV−visible absorption spectra of these monolayers on a quartz plate (Figure 2) well coincided with those for 6Az10-PVA,[20] further implying the identical quality of the monolayers. The deuterated polymer, 6Az10-PVA-d_3, differs from 6Az10-PVA in the molecular weight of

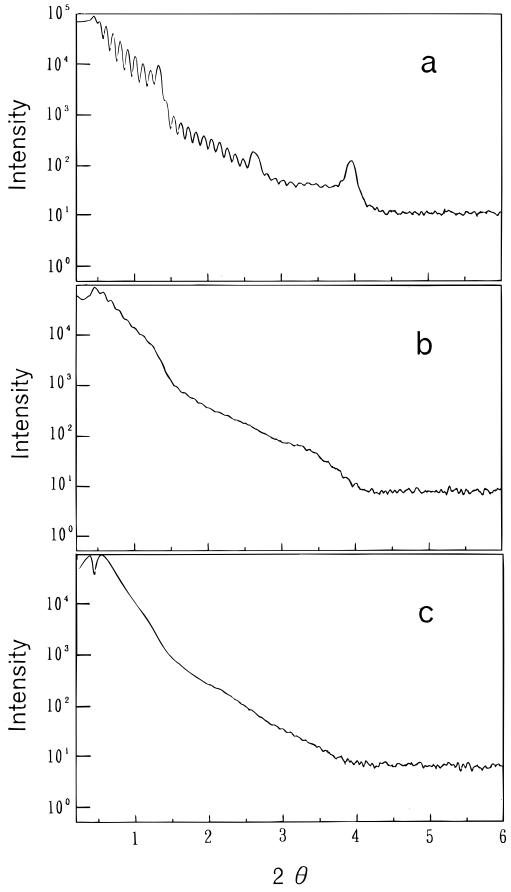

Figure 3. Small angle X-ray reflection patterns of 25-layered film A (a), film B (b), and film C (c) on a quartz plate.

the polymer of the main chain. The degrees of polymerization were ca. 2200 and ca. 500 for 6 Az10-PVA-d_3 and 6Az10-PVA, respectively. However, the difference in the molecular weight hardly affected the quality of the monolayers. We suppose that the structures of LB films prepared from 6Az10-PVA-d_3 and 6Az10-PVA monolayers are essentially identical.

3.2. Layer Structure Observed by X-ray Reflectometry. The film structure in terms of the assembled layer architecture and surface roughness was found to be influenced substantially by changes in the lateral packing density. Figure 3 indicates the small angle X-ray reflection profiles from 25-layered LB films of films A−C on a quartz plate. Film C was transferred in the *cis* form and then converted to the *trans* form by being kept in the dark at room temperature for 5 days. For film A, the reflection pattern exhibited clear Bragg peaks corresponding to the spacing of the periodical double monolayers which is overlapped with the oscillation pattern (Kiessig fringes) that originates from the interference of partial waves reflected at the air−film and film−substrate interfaces (Figure 3a). This indicates that film A bears a well-defined layer structure with a homogeneously smooth surface, as has been reported for other Az-containing polymers such as poly(L-glutamate)s,[1,2] polyacrylates,[3] and poly(hydroxyethyl acrylate)s.[4] In contrast, the structure of the more loosely packed films (films B and C) became considerably disordered. Film B exhibited insufficient Kiessig fringes with no Bragg peaks (Figure 3b), and moreover, film C gave no substantial diffraction peaks (Figure 3c). Thus, it is concluded that the relatively small decrease in the packing density reduced the lamellar order and the surface smoothness of the LB films in crucial manners.

Table 1. Structural Data from X-ray Reflectometry

LB films[a] (conditions)	overall thickness[b]/nm	spacing per monolayer[c]/nm
film A		
(initial *trans*)	85.1	3.7
(UV irrad)	83.7	
(vis irrad)	88.7	
(annealed[d])	85.4	(ca. 4)[e]
film B		
(initial *trans*)	78.5	
(UV irrad)	71.5	
(vis irrad)	81.5	
film C		
(initial *trans*)		

[a] 25 monolayers on a quartz plate. [b] Determined from Keissig fringes. [c] Determined from Bragg peaks. [d] At 80 °C for 12 h. [e] Very broad.

Table 1 summarizes the parameters, the total film thickness, and the spacing corresponding to the monolayer obtained from the X-ray reflection data. This table includes results taken before and after UV light irradiation, visible light irradiation, and a successive annealing procedure (80 °C for 12 h). The difference in the packing densities led to variation in the total thickness at the initial *trans* state. The overall film thicknesses of 25-layered films A and B were 85.1 and 78.5 nm, respectively.

Upon UV light irradiation, the overall film thickness decreased for both films A and B. This decrease in the film thickness mostly likely stems from a photoinduced tilt and a disorder of the Az side chain. The magnitude of the thickness decrease was larger for film B (78.5 → 71.5 nm, namely 8.9% reduction) than for film A (85.1 → 83.7 nm, 2.5% reduction), although the photoisomerization proceeded equally in these two LB films. It is anticipated that the more loosely packed film allows larger segmental mobility of photoinduced structural changes in the LB films. The overall film thickness increased again upon visible light irradiation. The thickness almost reverted to the initial value after visible light irradiation. It may be pointed out that the visible light irradiated films are even thicker than the initial state by approximately 3 nm. Following annealing, the film thickness returned to the original value (see values of film A, 85.4 from 85.1 nm). It can be stated, in any event, that the photo-effected changes in the overall film thickness are reversible processes.

On the contrary, the periodical layer structure was not reproducible once the film was exposed to light. After UV light irradiation, the Bragg peaks of film A disappeared, and they were not reproduced after exposure to visible light. The photoinduced process lowered the order of the lamellar structure while maintaining smoothness of the surface. Annealing of the film gave a very broadened Bragg peak corresponding to almost the original spacing. Essentially the same observations demonstrating disappearance of Bragg peaks by UV light illumination were already reported by other investigators using other Az side chain polymers.[2−4]

3.3. FT-IR Observation of the PVA Main Chain. Polarized transmission FT-IR spectra of 51-layered film A deposited on both sides of a CaF_2 plate are presented in Figure 4 as typical examples. The figure contains two spectra observed with polarization parallel (solid curve) and orthogonal (dotted curve) to the dipping direction. The C−D symmetric and antisymmetric stretching bands were observed at 2150 and 2220 cm^{-1},

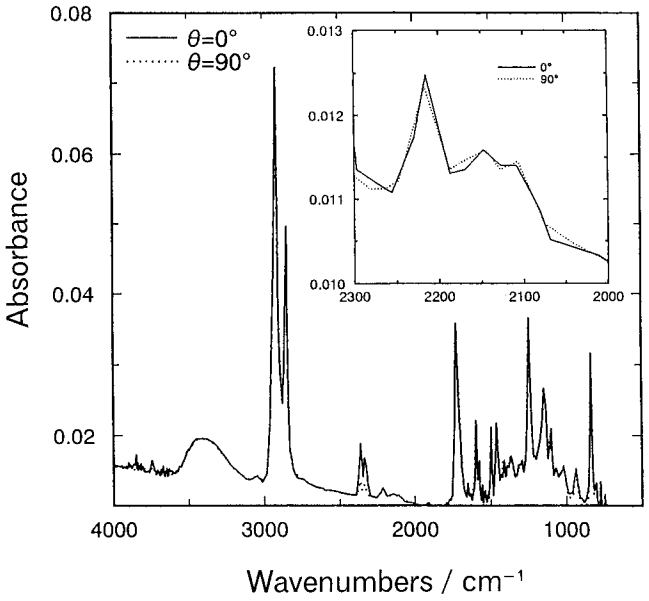

Figure 4. Transmission-polarized FT-IR spectra of 51-layered LB film A. Solid and dotted lines indicate spectra taken with the polarized beam set parallel (0°) and orthogonal (90°) to the dipping direction, respectively, in normal incidence. The inset of the figure displays the enlarged spectra of the C−D stretching band region.

Table 2. Band Assignments of 6Az10-PVA-d_3 Samples in the *Trans* State

wavenumber/cm^{-1}			
KBr pellet	cast film	LB film[a]	assignment
2926	2925	2924	CH_2 asym stretch ($\nu_{as}(CH_2)$)
2854	2854	2853	CH_2 sym stretch ($\nu_a(CH_2)$)
2213	2213	2213	CD_2 asym stretch ($\nu_{as}(CD_2)$)
1732	1732	1732	C=O stretch (ν(C=O))
1602	1602	1601	benzene ring C−C stretch (ν_{8a})
		1583	benzene ring C−C stretch (ν_{8b})
1501	1501	1501	benzene ring C−C stretch (ν_{19a})
		1481	benzene ring C=C stretch (ν_{19b})
		1466	CH_2 asym bend
1251	1251	1251	benzene ring −O−C asym stretch
840	841	841	benzene ring C−H out of plane

[a] 51-layered film A.

respectively. The inset of the figure shows the enlarged spectra of the C−D stretching band region. As it turned out in these measurements, no appreciable difference was observed between the two spectra within experimental error. Absence of the in-plane dichroic nature manifests that the orientation of the PVA backbone is highly random. Films B and C, more loosely packed films, gave virtually identical results in regard to the in-plane anisotropy of the C−D stretching absorption.

3.4. FT-IR Observation of Photoinduced Changes in the Az Side Chain. We subsequently focused our efforts on observations of light-induced structural and orientational modifications of the Az side chain by FT-IR spectroscopy. Since the photoisomerization of the Az unit causes a large shape change between the rodlike and the bent structures of this unit, photoinduced structural and orientational changes of the side chain in the films are anticipated. Assignments of the IR absorption bands for 6Az10-PVA-d_3 are summarized in Table 2 for three samples, a powder in the KBr pellet, a solvent-cast film, and an LB Film (films A).

Figure 5 displays the FT-IR spectra in the C−H stretching region of three 6Az10-PVA-d_3 samples, i.e., a powder sample in the KBr pellet (a), a cast film from a chloroform solution (b), and the 51-layered LB film (film A) (c), observed in the normal incidence. Each part involves spectra measured in the initial *trans* state (broken line) and after UV illumination (solid line). The UV illumination was performed for 20 min, within which the *trans*/*cis* photostationary state was reached (*cis* content, ca. 0.6). Although the *trans* → *cis* photoisomerization proceeded equally to the above content in the three samples, only the LB film exhibited an obvious decrease in the absorbance upon UV illumination (Figure 5c). The solvent-cast film and the KBr pellet showed virtually no spectral changes (Figure 5a,b). This difference can be interpreted as the consequence of the difference in the orientational order of the hydrocarbon chain with respect to the substrate plane. Considering the direction of the transition moment of the C−H stretching band, which is perpendicular to the direction of the alkyl chain, the UV light induced decrease in absorbance observed for the LB film should be ascribed to a photoinduced tilt of the hydrocarbon parts involving either or both the tail and spacer from the surface normal. Hydrocarbon chains in the solvent-cast film and the powder in a KBr pellet, on the other hand, should be randomly oriented, and hence the photo-

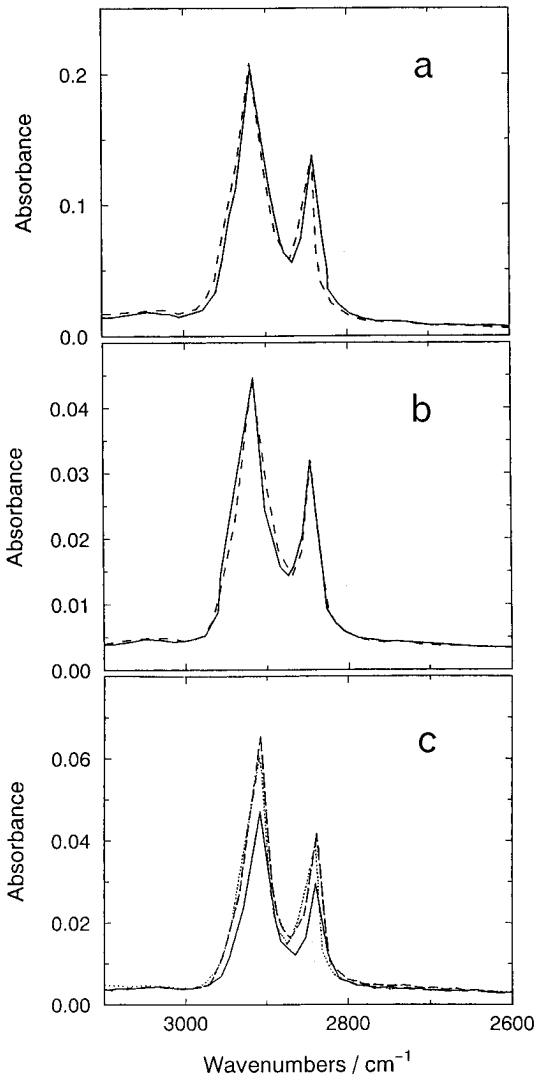

Figure 5. Transmission FT-IR spectra in the C−H stretching region of 6Az10-PVA-d_3 taken as the powder in a KBr pellet (a), the cast film from a chloroform solution (b), and 51-layered LB film A (c). Solid, broken, and dotted lines indicate the initial *trans*, UV light irradiated, and successive visible light irradiated states, respectively.

Table 3. Frequency and Absorbance Changes for Representative IR Bands in the LB Film (Film A) upon Photoirradiation

IR band	initial *trans* freq[c] (abs[d])	UV irrad[a] freq[c] (abs[d])	vis irrad[b] freq[c] (abs[d,e])
$\nu_{as}(CH_2)$	2924 (5.89)	2926 (4.90)	2924 (5.33)
ν(C═O)	1732 (2.62)	1730 (2.34)	1732 (2.44)
benzene ring ν_{19a}	1501 (1.03)	1501 (2.04)	1500 (2.46[f])

[a] After UV light (365 nm) irradiation. [b] After successive visible light (436 nm) irradiation. [c] Frequency of the band peak in wavenumbers (cm^{-1}). [d] Absorbance ($\times 10^{-2}$). [e] Absorbance taken immediately after the visible light irradiation. [f] This value reverted to the initial value (ca. 1×10^{-2}) after several days in the dark.

induced reorientation of the alkyl chain was not observed in the overall IR signal.

With respect to the LB film, representative IR absorption bands and their absorbances before and after light irradiation are listed in Table 3. As stated above, UV light illumination led to a decrease in the absorbance of the $\nu_{as}(CH_2)$ band from 0.059 to 0.049. Following illumination of the LB film with visible light, the intensity of this band reverted almost to the original level, although not completely. A frequency shift from 2924 to 2926 cm^{-1} of the $\nu_{as}(CH_2)$ band peak was observed upon UV light illumination. This frequency shift to the higher wavelengths is due to an increase in the *gauche* conformer in the alkyl chain.[21,24] Similarly to the absorbance changes, the position of the band peak turned back again to the initial frequency upon exposure to visible light. These data imply that the photoinduced orientational and conformational changes of the hydrocarbon chains are reversible. The photoinduced decrease in the overall film thickness (section 3.2) can be interpreted to involve contributions of both the tilt of the side chain and conformational disorder in the alkyl chain.

In contrast, the reversibility of the photoinduced changes in the IR band of the aromatic ring, ν_{19a} at 1500−1501 cm^{-1} was found to be poor (see Table 3). Irradiation with UV light brought about an increase of the absorbance from 0.0103 to 0.0204. Since the direction of the transition moment of this band is almost parallel to the long axis of the Az unit, the enhancement of the absorbance is in agreement with a picture that UV light induces bending of the perpendicularly oriented *trans*-Az unit. However, the absorbance recovery of this band required several days in the dark. In this manner, the structural changes of the overall side chain are not monotonous.

The absorbance of the C═O stretching band remained constant during this process. This can be ascribed to a large distance from the Az moiety due to the long spacer and more likely to a reduced mobility caused by the directly attached PVA backbone.

3.5. On the Rate of Photoinduced Structural Changes of the LB Film. Figure 6 indicates the time profile of absorbance changes at three characteristic bands shown in Table 2, $\nu_{as}(CH_2)$, ν(C═O), and benzene ring ν_{19a}, upon UV illumination using a 150-W xenon lamp for film A. A careful comparison of the time profile for film A led to a finding that the absorbance changes of the C−H stretching band proceed more slowly than that of the benzene ring ν_{19a} band. Table 4 lists the apparent first-order rate constant (k/s^{-1}) estimated by the IR absorbance changes of films A−C. As seen from the table, k obtained at the ν_{19a} stretching band was constant for the three LB films ($k = 1.0-1.1$ s^{-1}), but there was an appreciable rate reduction in k for the ν_{as}-

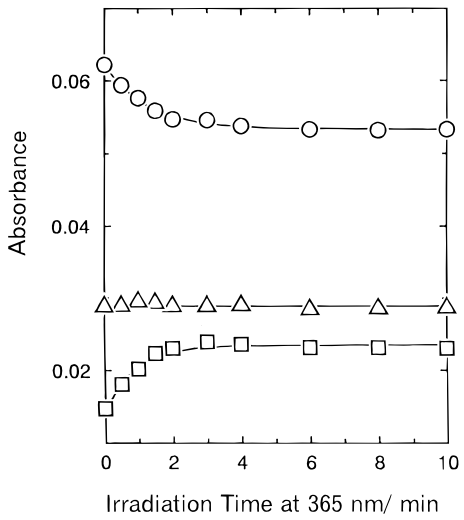

Figure 6. Time profiles of absorbance changes of $\nu_{as}(CH_2)$ (circles), benzene ring ν_{19a} (squares), and ν(C═O) (triangles) bands for 51-layered LB film A on a CaF_2 plate upon UV light illumination.

Table 4. Apparent First-Order Rate Constant of the IR Signal Changes and the Response Time of the Nematic LC upon UV Light Illumination

designation	$k[\nu_{as}(CH_2)]$[a]/ s^{-1}	$k[\nu_{19a}]$[a]/ s^{-1}	LC response time[b]/min
film A	0.78	1.09	9.7
film B	1.24	1.12	7.5
film C	1.22	1.19	3.7

[a] $k[\nu_{as}(CH_2)]$ and $k[\nu_{19a}]$ were estimated by monitoring absorbance changes of $\nu_{as}(CH_2)$ and benzene ring ν_{19a} bands, respectively, on the continuous illumination with 365 nm light at the exposure energy of 0.9 mW cm^{-1}. [b] Response time of the LC alignment changes defined as the required time for 90% change of the total; see arrows in Figure 7.

(CH_2) band only in film A ($k = 0.78$ s^{-1}). As expected, the time constant of UV light induced changes of the ν_{19a} band coincided with that of the electronic spectral changes in the $\pi-\pi^*$ band of the Az chromophore. For the more loosely packed films, films B and C, the ν_{as}-(CH_2) and ν_{19a} bands changed concurrently.

3.6. Alignment Changes of a Nematic LC. A nematic LC, DON-103, was sandwiched between the substrate modified by a 6Az10-PVA-d_3 LB monolayer and an OTS-modified substrate (cell gap 8 μm). UV light illumination of this LC cell induced the homeotropic → planar alignment change. The alignment response was monitored by observing the absorbance changes of a dichroic dye (LCD-118, Nippon Kayaku) doped in the LC phase. The profiles of UV light induced absorbance changes of the dichroic dye are shown in Figure 7. The response times, which are defined as the time required for the 90% change of the total, the arrows in the figure, are summarized in Table 4. As clearly shown here, the response time was prolonged with an increase in the lateral Az packing density. Thus the Az packing density influenced not only the structure of the LB films themselves but also the commanding ability of LC molecule alignment. It is worthwhile to note here that UV light induced LC alignment started to occur after a majority of the Az chromophore was already photoisomerized to the *cis* form. The alignment change of the LC molecules is not a concurrent but delayed process from the movement of the Az side chain of the LB film (cf. Figures 6 and 7).

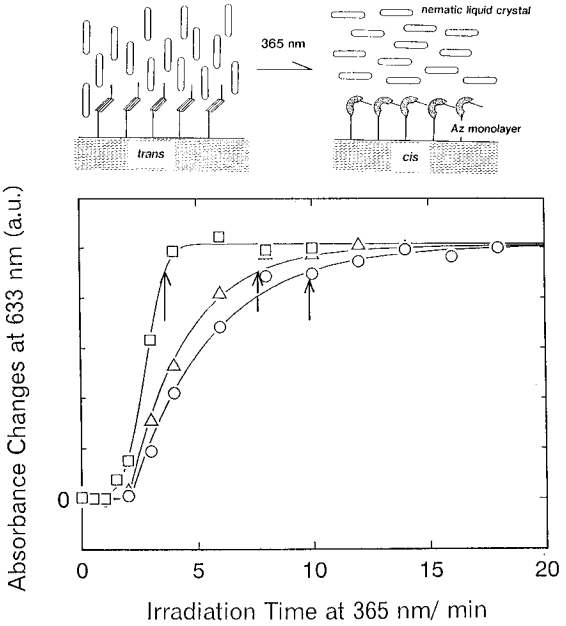

Figure 7. Time courses of absorbance changes of a dichroic dye upon UV light illumination reflecting homeotropic → planar alignment changes of a DON-103 nematic LC induced by the *trans* → *cis* photoisomerization of 6 Az10-PVA-d_3 LB monolayers. Circles, triangles, and squares represent data for film A, film B, and film C, respectively. Arrows indicate the time points required for a 90% change of the total. The drawing above the figure shows a schematic illustration of the UV light induced alignment change of a nematic LC placed on the Az LB monolayer.

4. Discussion

4.1. The Film Structure Depending on the Lateral Packing Density. To our knowledge we present for the first time the critical changes of the Az LB film structure affected by the lateral packing density. The lateral packing density can be modified by changing both the amount of introduced Az side chain (concerning the primary structure of the polymer) and the interfacial compression during the LB process (regarding the higher-order structure). This study indicates at least the crucial importance of the conditions of the LB deposition for the assembled structure of the LB film. Sawodny et al.[3] studied structural and optical properties of LB films composed of an Az homopolymer and discussed the merit of using a homopolymer to obtain the concentration of optically functional chromophore in the LB films. However, judging from the formation of the well-structured LB films in film A, we suppose that our copolymer that contains only 24% Az chromophore in the main chain is able to form LB films possessing the comparable structure, provided that it is sufficiently compressed laterally at the air−water interface on LB deposition. Az LB films hitherto reported have well-defined lamellar periodicity and smooth surfaces. These films are typically prepared at high surface pressures around 30 mN m^{-1}. It may be assumed that well-defined Az LB films require sufficient compression of monolayers at the air−water interface.

Complete disappearance of Kiessig fringes and Bragg peaks for the film of the most loosely packed film (film C) conveys that this film deserves morphological observations. In this context, we have started morphological examinations of Az LB films by means of the dc plasma polymerization replica film method (PPR technique).[25] The replicated polymer film is observed by a transmission electron microscope. The PPR technique is a particularly powerful tool for morphological observations of soft samples such as living organs and organic thin films having an image resolution of 0.6 nm. In a preliminary experiment, the surface of 9-layered film C was found to be rugged and showed characteristic arrayed projections with diameters of ca. 0.4 μm (unpublished results). This justifies the absence of Kiessig fringes and also the Bragg peaks. Films A and B should have more smooth surfaces, judging from the X-ray data. It is thus anticipated that changes in the lateral packing density lead to morphological changes at the micrometer level. The PPR experiments in this regard are now in progress.

4.2. On the Orientation of the PVA Main Chain. The in-plane orientation of the nematic LC molecule on the 6Az10-PVA LB monolayer is found to be dependent on the Az packing density. Our previous report[20] demonstrated that there is an orientational inversion in the homogeneous alignment of the LC from parallel to orthogonal with respect to the dipping direction between films A and B. Nevertheless, we did not observe any appreciable in-plane orientational preference of the PVA-d_3 main chain in the LB film at the three Az packing densities examined. It would be assumed that these conflicting results are due to the following two possibilities: (i) The orientational origin is possessed only by the side chain, and (ii) the dichroic ratio due to the backbone orientation is beyond the experimental accuracy. We assume at the moment that the latter explanation is more conceivable on the ground that the Az LB film has a memory effect regarding the inplane LC orientation. Even though the in-plane orientation was changed by the linearly polarized UV light irradiation,[26] the acquired orientation again reverted to the original direction imposed by the dipping process after a couple repetitions of alternating nonpolarized visible and UV light illumination for both 6Az10-PVA and 6Az10-PVA-d_3 (unpublished results). Sekkat et al.[23] demonstrated this memory effect by surface plasmon resonance waveguide spectroscopy using the 6Az10-PVA monolayered LB films. Appearance of such an orientational memory effect would be more naturally understood by assuming a preferred orientation of the polymer backbone.

4.3. Photoinduced Structural Changes of Az LB Films. The important point deduced from the FT-IR observations is that the segmental motion at the alkyl part is not necessarily concurrent with that of the aromatic Az part. The retarded motion of the alkyl parts compared with that of the aromatic moiety upon UV light irradiation observed for film A seems to be the consequence of its environmental restriction. It seems, furthermore, that this is correlated with the smaller decrease in the overall thickness of film A upon UV light illumination. The discrepancy in the local motion became more obvious in the reverse process on visible light irradiation. The intensity of the $\nu_{as}(CH_2)$ band in the FT-IR spectrum reverted immediately to the initial level, but that of the ν_{19a} band required approximately 1 week to reach the original state. These biphasic molecular processes may be associated with the structural features that the overall thickness is photochemically reversible whereas the local lamellar layer structure is irreversibly destroyed.

Sawodny et al.[3] and Menzel et al.[2] both reported that the overall film thickness is unchanged before and after UV light irradiation for their Az LB films. We regard films A and B in this study as the first examples that

exhibited changes in the total film thickness upon light illumination. Yet, it seems to be difficult to figure out why only our LB films showed the macroscopic changes reflected in the film thickness. One possible explanation that could be offered is the difference in the ratio of the introduced Az side chain: Sawodny and Menzel utilize homopolymers, and our materials are statistic copolymers containing 24% of the side chain. Copolymers could allow larger mobility of the side chain which leads to macroscopic thickness changes.

The transfer step of the molecular information from the Az LB film to nematic LC molecules was even more largely influenced by the lateral packing density. An increase in the packing density substantially retarded the rate of homeotropic → planar LC alignment changes. The motional retardation of the alkyl chain in the Az side chain was not detectable in comparison of films B and C. Nevertheless, a substantial difference was observed between them in the response time of LC alignment changes (see Table 4). It may be deduced from these data that the time retardation becomes larger in the LC reorientation than in the reorientation of the alkyl part of the Az side chain because the former is driven by the intermolecular interaction and the latter takes place through the covalently linked spacer. Close packing of the surface layer possibly prevents LC molecules from penetrating into the Az side chain array, leading to less effective interaction between the command layer and the LC molecules.

5. Conclusion

It is found here that considerable structural variations of PVA-based Az LB films occur through changes in the lateral packing density. The X-rays analysis indicated that the more densely packed film had the better-structured LB films in terms of the order of the lamellar structure and the surface smoothness. We could not succeed in obtaining proper information on the orientation of the deuterated PVA main chain due to too small IR signals of C−D stretching bands. Nevertheless, some important knowledge was obtained on the structural and dynamic nature of the Az side chain, as follows: (i) UV light illumination induced a tilt and disorder of the side chain, which was possibly reflected by the changes in the total film thickness. (ii) Within the side chain, inconsistency in the time constants of the photoinduced changes at the alkyl and aromatic parts was observed for the most densely packed LB film, the motion of the alkyl part being delayed from that of the aromatic Az part. (iii) The retardation in the time constant was more obvious in the motion of alignment changes of LC molecules driven by these Az LB films. In these manners, the previous[20] and this works present the importance of the parameter of the lateral packing density in terms of making structures of LB films, affecting the dynamic nature of photoinduced modifications, and consequently its aligning ability of LC molecules at the command surface.

Acknowledgment. We thank Prof. K. Sakota of the Research Institute for Electronic Science at Hokkaido University for his generous donation of a deuterated PVA.

References and Notes

(1) Menzel, H.; Weichart, B.; Hallensleben, M. L. *Thin Solid Films* **1993**, *223*, 181.
(2) Menzel, H.; Weichart, B.; Schmidt, A.; Paul, S.; Knoll, W.; Stumpe, J.; Fischer, T. *Langmuir* **1994**, *10*, 1926.
(3) Sawodny, M.; Schmidt, A.; Stamm, M.; Knoll, W.; Urban, C.; Ringsdorf, H. *Polym. Adv. Technol.* **1991**, *2*, 127.
(4) Möbius, G.; Pietsch, U.; Geue, Th.; Stumpe, J.; Schuster, A.; Ringsdorf, H. *Thin Solid Films* **1994**, *247*, 235.
(5) Nishiyama, K.; Kurihara, M.; Fujihira, M. *Thin Solid Films* **1989**, *179*, 477.
(6) Yokoyama, S.; Kakimoto, M.; Imai, Y. *Thin Solid Films* **1994**, *242*, 183.
(7) Maack, J.; Ahuja, R. C.; Tachibana, H. *J. Phys. Chem.* **1995**, *99*, 9219.
(8) Tachibana, H.; Nakamura, T.; Matsumoto, M.; Komizu, H.; Mannda, E.; Niino, H.; Yabe, A.; Kawabata, Y. *J. Am. Chem. Soc.* **1989**, *111*, 3080.
(9) Liu, Z. F.; Hashimoto, K.; Fujishima, A. *Nature* **1990**, *347*, 658.
(10) Nakahara, H.; Fukuda, K. *J. Colloid Interface Sci.* **1983**, *93*, 530.
(11) Nakahara, H.; Fukuda, K.; Shimomura, M.; Kunitake, T. *Nippon Kagaku Kaishi* **1988**, 1001.
(12) Shimomura, M.; Kunitake, T. *Thin Solid Films* **1985**, *132*, 243.
(13) Penner, L.; Schildkraut, J. S.; Ringsdorf, H.; Schuster, A. *Macromolecules* **1991**, *24*, 1041.
(14) Kawai, T.; Umemura, J.; Takenaka, T. *Langmuir* **1990**, *6*, 672.
(15) Sato, T.; Ozaki, Y. *Langmuir* **1994**, *10*, 2363.
(16) Seki, T.; Ichimura, K. *Polym. Commun.* **1989**, *30*, 108.
(17) Seki, T.; Ichimura, K. *Thin Solid Films* **1989**, *179*, 77.
(18) Seki, T.; Sakuragi, M.; Kawanishi, Y.; Tamaki, T.; Fukuda, R.; Ichimura, K. *Langmuir* **1993**, *9*, 211.
(19) Ichimura, K.; Seki, T.; Kawanishi, Y.; Suzuki, Y.; Sakuragi, M.; Tamaki, T. In *Photo-reactive Materials for Ultrahigh Density Optical Memory*; Irie, M., Ed.; Elsevier: Amsterdam, 1994; pp 55−83.
(20) Seki, T.; Fukuda, R.; Tamaki, T.; Ichimura, K. *Thin Solid Films* **1994**, *243*, 675.
(21) Katayama, N.; Ozaki, Y.; Seki, T.; Tamaki, T.; Iriyama, K. *Langmuir* **1994**, *10*, 1898.
(22) Knobloch, H.; Orendi, H.; Büchel, M.; Seki, T.; Ito, S.; Knoll, W. *J. Appl. Phys.* **1995**, *77*, 481.
(23) Sekkat, Z.; Buchel, M.; Orendi, H.; Knobloch, H.; Seki, T.; Ito, S.; Koberstein, J.; Knoll, W. *Opt. Commun.* **1994**, *111*, 324.
(24) Sapper, H.; Cameron, D. G.; Mantsch, H. H. *Can. J. Chem.* **1981**, *59*, 2543.
(25) Tanaka, A.; Yamaguchi, M.; Iwasaki, T.; Iriyama, K. *Chem. Lett.* **1989**, 1219.
(26) Kawanishi, Y.; Tamaki, T.; Sakuragi, M.; Seki, T.; Suzuki, Y.; Ichimura, K. *Langmuir* **1992**, *8*, 2601.

MA951268R